


Refinement of Housner's model on rocking blocks

Tamás Ther¹  · László P. Kollár²

Received: 21 December 2015 / Accepted: 8 November 2016 / Published online: 18 November 2016
© European Union 2016

Abstract Housner published a simple model for the rocking block more than five decades ago (Housner in Bull Seismol Soc Am 53:403–417, 1963), which is widely used also for modeling stone and masonry columns and arches. In this paper we investigate the reasons of the well-known fact that experiments show lower energy loss during impact than it is predicted by Housner's model. It was found that a reasonable explanation for the difference is that in the original model the best case scenario was assumed: that impact occurs at the edges, which results in the maximum energy loss. In reality, due to the unevenness of the surfaces, or due to the presence of aggregates between the interfaces, rocking may occur with consecutive impacts, which reduces the energy loss. This hypothesis was also verified by experiments.

Keywords Rocking block · Rigid block · Housner · Impact

1 Introduction

Housner published his classical paper more than five decades ago (Housner 1963), in which he presented a simple model for the rocking block (Fig. 1). He investigated a block which rotates around corner *A*, then—when the block reaches the vertical position—impact occurs, and the block rotates further around corner *B*. Assuming identical angular

✉ Tamás Ther
ther@szt.bme.hu

László P. Kollár
lkollar@eik.bme.hu

¹ Department of Mechanics, Materials and Structures, Budapest University of Technology and Economics, Műegyetem rkp. 1-3, 1111 Budapest, Hungary

² Department of Structural Engineering, Budapest University of Technology and Economics, Műegyetem rkp. 1-3, 1111 Budapest, Hungary

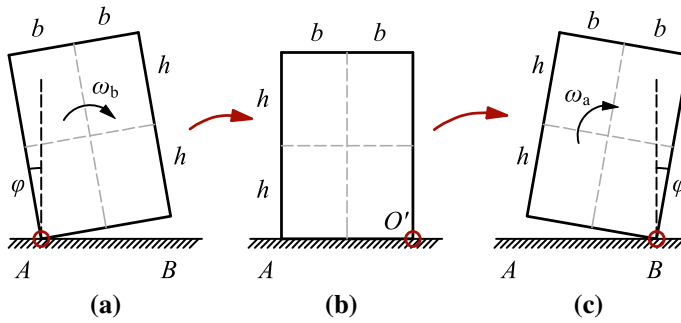


Fig. 1 Housner's model for a rocking block

momentum on corner *B* before and after the impact (Fig. 1), he determined the angular velocity after impact, ω_a (Fig. 1c) as a function of the geometry and the angular velocity before impact, ω_b (Fig. 1a), see Eq. (1).

Housner's model is a very important element of the analysis of structures subjected to earthquakes, where cracks may open and close during excitations. These are, for example: columns, walls and arches made of masonry, stone or unreinforced concrete blocks (Fig. 2).

The square of the angular velocity is proportional to the kinetic energy of the rocking block, and hence at every impact there is an energy loss. The motion of a rocking block—subjected to gravity load only—according to Housner's model is shown in Fig. 3. Note that both the amplitude and the time between impacts decrease with time.

The rocking block was investigated experimentally by several researchers: (Anooshehpour and Brune 2002) used timber blocks, Prieto-Castrillo (2007) granite, Aslam et al. (1980) and Ma (2010) concrete, Lipscombe and Pellegrino (1993) used steel elements. In almost every case it was found that in the experiments the energy loss (and the decrease in angular velocity) is smaller than the one predicted by Housner's model (Fig. 3). The results are shown in Table 1 and in Fig. 4 (the angular velocity ratio, μ is defined as the ratio of the angular velocities after and before impact, while the loss of kinetic energy, η as the change in kinetic energy during impact over the kinetic energy before impact).

In case of the experiments of Elgawady et al. (2011) rocking did not occur freely but through a steel mechanism, which was applied on the system. This is the reason that this

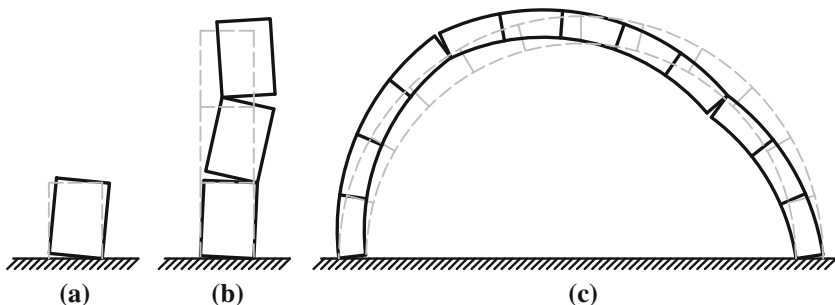


Fig. 2 Columns and arches, where Housner's model is applied

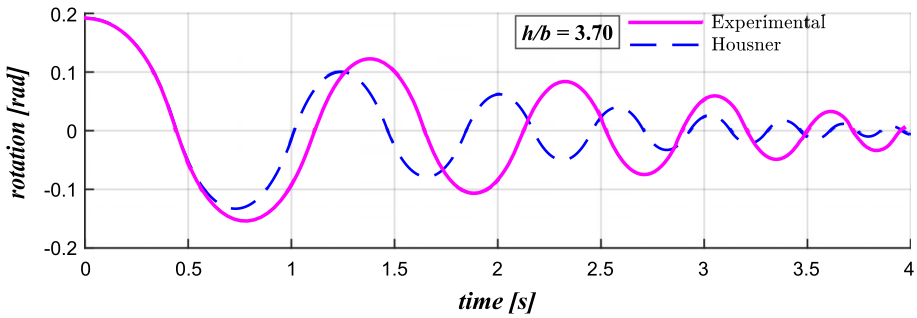


Fig. 3 Typical time-displacement curve of a rocking block according to Housner’s model (dashed line), and according to our experiment (solid line)

Table 1 Experimental results (Ogawa 1977; Prieto 2007; Elgawady et al. 2011) compared with Housner’s model. η_{Hous} is the relative energy loss

Author	Material of the block	$2h$	$2b$	$2b_2$	h/b	Loss in energy	
						$\bar{\eta}$ (%)	η_{Hous} (%)
Ogawa (1977)	Timber	200	100		2.00	37.6	51.0
Ogawa (1977)	Timber	300	100		3.00	22.6	27.8
Ogawa (1977)	Timber	400	100		4.00	11.6	16.9
Aslam et al. (1980)	Concrete block with aluminum plate	771.5	152		5.08	14.4	10.9
ElGawady et al. (2011)	Concrete block with steel plate	950	190		5.00	15.6	11.2
Prieto (2007)	Granite	1000	250		4.00	12.4	16.9
Prieto (2007)	Granite	1000	170		5.88	5.3	8.2
Prieto (2007)	Granite	1000	120		8.33	4.4	4.2
Prieto (2007)	Granite	500	246	160	2.03	14.0	25.2

η_{Hous} was calculated by Eqs. (1) and (11) except the last one, where Eqs. (6) and (11) were used

experiment was not included in Fig. 4. Aslam et al. (1980) reported high slips (and, accordingly, high energy loss) during the experiments, which explains that in this case the energy loss is higher than in case of Housner’s model.

Researchers gave different explanations for the significant differences between the results of the experiments and the model (see the summary of Lagomarsino 2015), and several improvements were suggested. Augusti and Sinopoli (1992) and Kounadis (2015) took into account the sliding between the block and the base, which, especially for small aspect ratios, is a necessary and important improvement. Note, however, that it cannot explain that the model underpredicts the energy loss (Table 1). A possible explanation assumes that the impact is neither plastic nor elastic: Lipscombe and Pellegrino (1993) stated that the bouncing is significant for short blocks. They insert the coefficient of restitution into Housner’s equations to reach an agreement with the experiments, where the bouncing of the element was detected. This effect has been experimentally tested by Elgawady et al. (2011), by investigating the material of the surface of the base under the rocking element. Ma (2010) ran over 400 experimental tests with a built-in steel mechanism that prevents sliding to explain the discrepancy. In conclusion, he stated that the

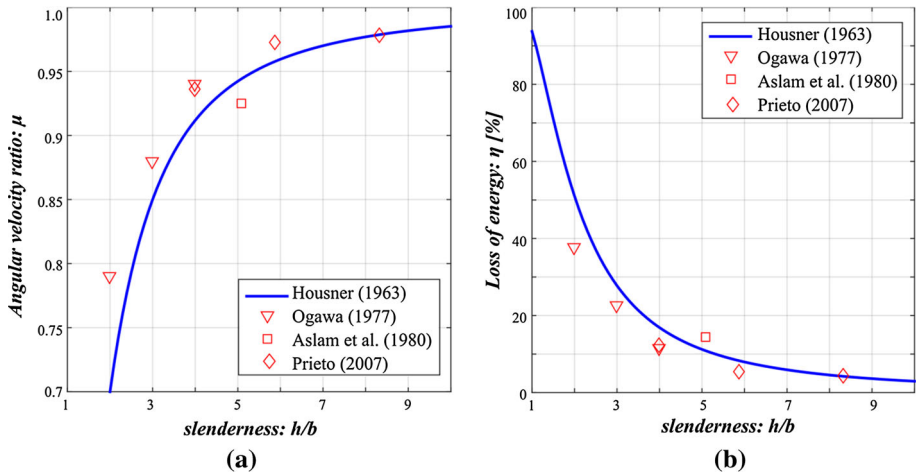


Fig. 4 The reduction in speed (μ) and the loss of kinetic energy ($\eta_{\text{Hous}} = 1 - \mu_{\text{Hous}}^2$) for different aspect ratios. Experimental results (Ogawa 1977; Aslam et al. 1980; Prieto 2007) compared with Housner’s model (Aslam reported significant slips, which explains the high energy loss)

experiments have demonstrated that despite the very simple appearance of free rocking motion, highly complex interactions play an important role. To overcome the differences between the model and the experiments, some of the researchers suggested to use an angular velocity ratio (μ) which agrees with the experiment and not with Housner’s model (Priestley et al. 1978; Aslam et al. 1980; Lipscombe and Pellegrino 1993; Anooshehpour and Brune 2002; Elgawady et al. 2011).

2 Problem statement

In his original paper Housner derived the following expression to calculate the angular velocity of the block after impact (Fig. 1c):

$$\omega_a = \mu_{\text{Hous}} \omega_b, \quad \mu_{\text{Hous}} = \frac{2h^2 - b^2}{2h^2 + 2b^2}, \tag{1}$$

where ω_b and ω_a are the angular velocities before and after rocking, h and b are the dimensions of the block, μ is the angular velocity ratio.

As we stated in the Introduction (see Figs. 3, 4) experiments show lower energy loss during impact than it is predicted by Housner’s model, which means that—as a rule—Housner’s model is unconservative. Although, in practice, fudge-factors may be successfully used to obtain proper results, it is worthwhile to find a physical explanation for the difference, and—if possible—to have an improved mechanical model.

Note that in spite of the presented inaccuracies Housner’s model is widely applied because of its simplicity and physical clarity. Numerical solutions were developed to follow the motion (Augusti and Sinopoli 1992; Lipscombe and Pellegrino 1993; Prieto et al. 2004; Kounadis 2015), and with the aid of these, several authors determined rocking spectra or stability maps to analyze the stability of a single rocking block (Housner 1963; Hogan 1989; Shi and Anooshehpour 1996; Psycharis et al. 2000; Makris and Konstantinidis 2003; Prieto 2007; Makris and Vassiliou 2012; Voyagaki et al. 2013). Oppenheim

(1992) extended this for the investigation of arches and De Lorenzis (2007) defined stability maps for impulse-ground motions. Housner’s model was also extended to investigate non-symmetric monolith blocks (Shi and Anooshehpour 1996; Di Egidio and Contento 2009; Zulli et al. 2012) and two (Psycharis 1990; Spanos et al. 2001) or multi degree of freedom structures (Ther and Kollár 2014).

Our aim in this paper is to give an explanation and to present a new model, which can be used not only for the rocking block, but also—as a building element—for the modeling of masonry and stone columns and arches (Fig. 2).

3 Hypothesis and approach

First, we apply a simple modification on Housner’s classical model. It is assumed that the surface of the block (or the ground surface) is not perfectly smooth, but there is a small bump (or aggregate) in the middle (Fig. 5a). In this case the rocking occurs with two impacts (Ther and Kollár 2014). Before rocking the block rotates around corner *A*. Then, impact occurs, and the

- Block rotates around point *C* (bump or aggregate). Following that a
- Second impact occurs and the block rotates around corner *B*.

If the size of the bump (or aggregate) is small the time between the two impacts is also small, however, the final angular velocity is higher than in Housner’s model (This can be shown simply by applying Housner’s model twice. See Eq. (10) in the “Appendix”).

If there are two bumps (Fig. 5b), rocking occurs with three impacts, and if there are n bumps (which form a convex surface), rocking occurs in $n + 1$ impacts. Figure 6 shows the loss in kinetic energy as a function of the aspect ratios with 1, 2, ..., 100 bumps. If the number of bumps goes to infinity, the block will “roll” and the energy loss is zero.

In reality, there is no perfect surface (Fig. 7a), and as it was shown above, even a small unevenness of the surface (bump or aggregate) changes the loss in the kinetic energy during rocking significantly.

It is assumed that the main reason that Housner’s model overpredicts the loss in kinetic energy is the following:

- Impact does not occur purely at the edges of the blocks (Fig. 7b), rather—in consecutive steps—at bumps and then at the edges (Fig. 7c).

It is suggested that Housner’s model can be improved by taking into account these additional impacts during rocking.

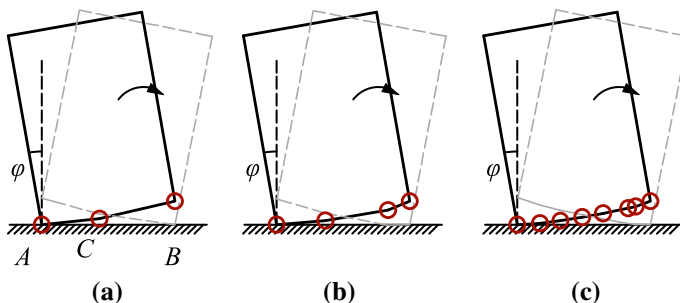


Fig. 5 Rocking block. **a** one bump in the middle, **b** two bumps, **c** several bumps

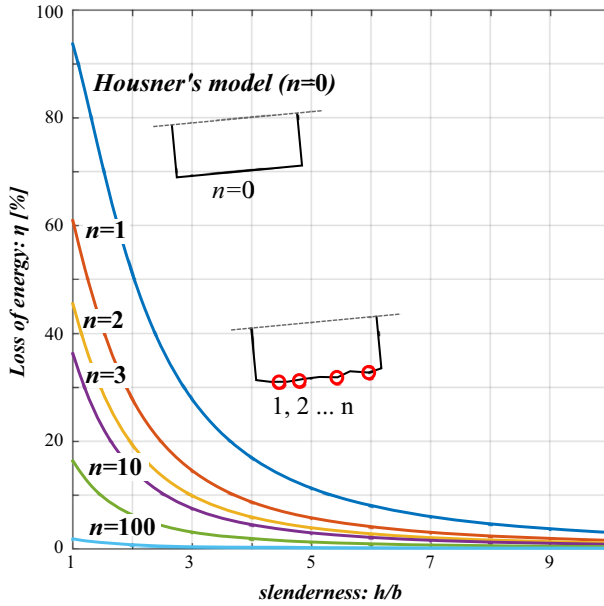


Fig. 6 Loss in kinetic energy as a function of slenderness of the block for n bumps

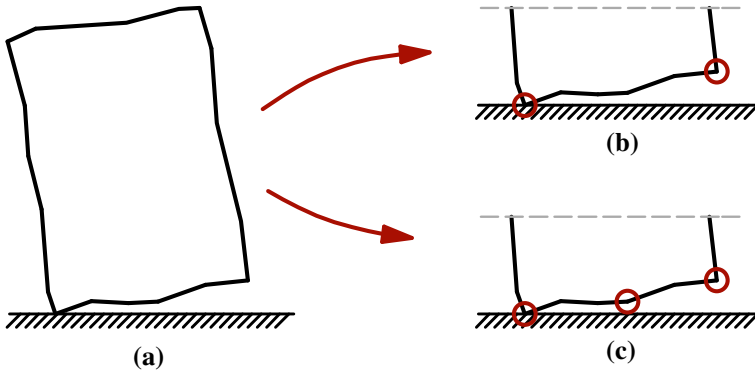


Fig. 7 Comparison of Housner’s model and the modification with an additional bump in the middle

To evaluate the above hypothesis experiments were carried out, which are presented in the next section. In addition, we investigated some of the experiments available in the literature.

4 Experiments

Two granite blocks were manufactured with different aspect ratios, shown in Fig. 8. (At two adjacent edges approximately 5×5 mm triangular prisms were cut off). The depth of the blocks was 300 mm to maintain the 2D rocking motion, since blocks with square cross

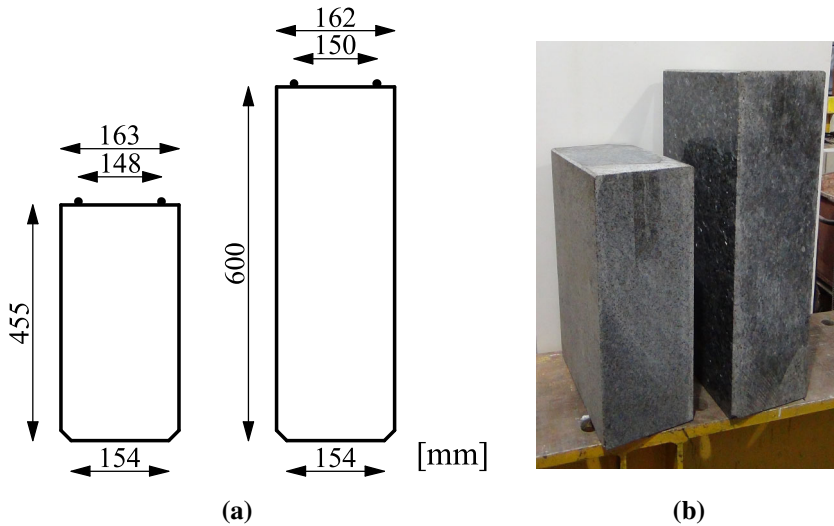


Fig. 8 Picture and the sizes of granite blocks used in the experiments

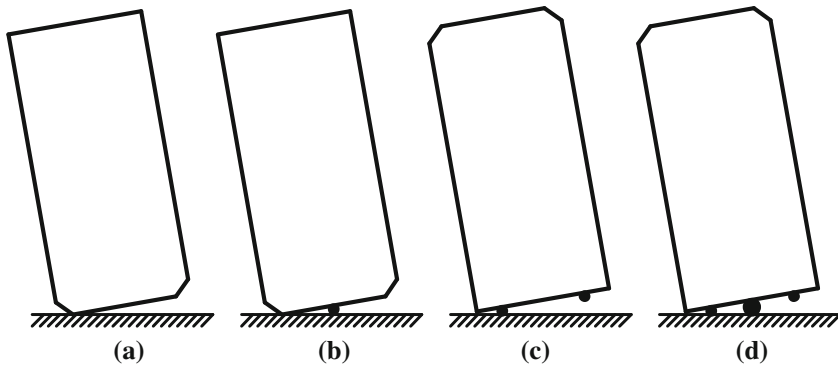


Fig. 9 Configurations of a block applied in the tests

sections, as it is reported in Zulli et al. (2012), may show 3D twisting motion. The rocking of each block was tested in 4 different configurations (Fig. 9a–d):

- (a) Rocking on the surface, where the corners are cut off,
- (b) Rocking on the same surface with a 2 mm diameter wire attached at the middle,
- (c) Two wires attached at the opposite surface, where two wires attached 7 mm from the edges,
- (d) An additional 4 mm diameter wire attached at the middle.

Note that the Young modulus of the steel is about 3–4 times bigger than that of the granite, hence the somewhat softer contact has only a minor effect. (Table 3, configuration c shows that the calculated, theoretical value of the energy loss—assuming inelastic impact—is 17.2%, while the measured value—due to the deformations and/or the slip is only a little bit higher: 19.5%. Our intention was to place the two wires at the same

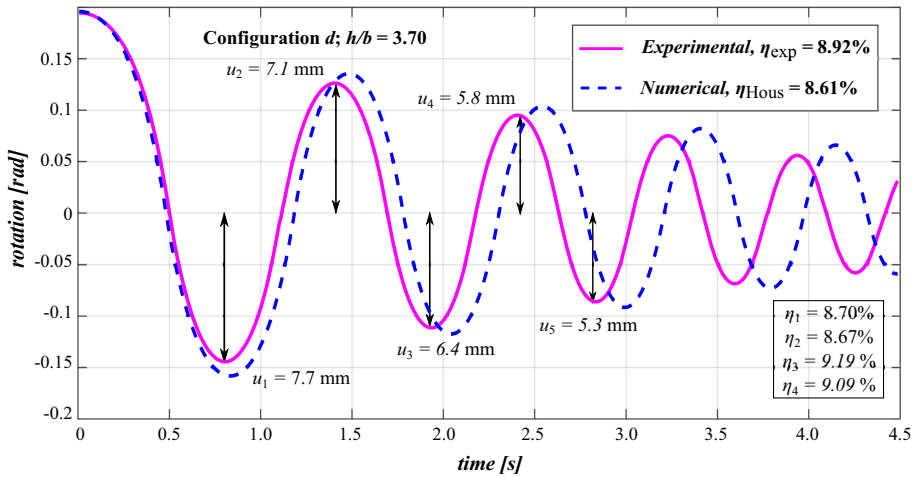


Fig. 10 Angle of rotation as a function of time, configuration d (the potential energy of the block was measured at the maximum amplitudes of the rotations marked with arrows)

distance as the width between the cuts, i.e. ~ 5 mm from the edges, however there is a small difference.) Configuration *a* basically agrees with Housner’s case with the slight modification that the axes of rotations are 5 mm from the edges of the blocks. The reduction in kinetic energy slightly changes as well, as discussed in the “Appendix” [see Eqs. (6) and (11)].

In case of configurations *b* and *d* two impacts occur during rocking; while in case of configuration *c* it is made sure that one impact occurs exactly at the chosen position defined by the wires close to the edges.

We ran each configuration 40 times, hence, the number of performed tests is 320. In each test a block was placed on a horizontal, 35 mm thick steel plate, the block was tilted close to its neutral position, and then it was moved by the gravity force (free rocking). The motion was measured by an x-IMU device with 256 Hz accuracy (for comparison, in a few cases one of the blocks were placed on top of the other granite block instead of the steel surface. The results of rocking were identical to those when rocking was performed on a steel plate).

A typical displacement (angle of rotation) curve as a function of time is given in Fig. 10 by solid line.

An important measure of the behavior of the system is the change in kinetic energy before and after each rocking. The system has kinetic and potential energy. The first one is zero when the vertical displacement is maximum, while the second one is taken to be zero when the angular rotation is zero, and hence the vertical displacement is minimum. As a consequence, by neglecting the energy loss between two consecutive impacts, the maximum kinetic energy is identical to the maximum potential energy (E_i). Thus E_i can be calculated by multiplying the maximum vertical displacement of the center of gravity by the weight of the block. The relative energy loss is calculated as

$$\bar{\eta}_i = \frac{E_i - E_{i+1}}{E_i} \approx \frac{u_i - u_{i+1}}{u_i}, \tag{2}$$

which is also shown in Fig. 10. In Eq. (2) u_i and u_{i+1} are the amplitudes of displacements before and after the i -th rocking. (We applied the “bar” to identify that $\bar{\eta}$ is obtained from

Table 2 Relative energy loss between adjacent rockings in the experiments ($\bar{\eta}$) and in Housner’s model [η_{HousC} , Eqs. (1), (6) and (11)]

Configuration	$\bar{\eta}$ Slenderness: h/b		η_{HousC} Slenderness: h/b	
	2.79	3.70	2.79	3.70
a	13.4 ± 3.0%	12.4 ± 0.9%	28.4%	17.7%

Table 3 The relative energy loss between adjacent rockings in the experiments ($\bar{\eta}$) and in the calculation (η_{HousC} for configuration c , and $\eta_{\text{HousC}}^{2\text{imp}}$ for configuration b and d)

The cases where the slip of the block just after impact was significant are marked by an asterisk

Configuration	$\bar{\eta}$ Slenderness: h/b		η_{HousC} & $\eta_{\text{HousC}}^{2\text{imp}}$ Slenderness: h/b	
	2.79 (%)	3.70 (%)	2.79 (%)	3.70 (%)
b	11.2 ± 1.2	6.9 ± 0.4	14.8	9.0
c	57.9*	19.5 ± 1.0	26.5	17.2
d	22.9*	8.8 ± 1.0	13.8	8.6

an experiment.) It is important to notice that with reasonable accuracy the values of $\bar{\eta}_i$ are identical at every rocking. $\bar{\eta}$ -s—calculated as the average of four consecutive $\bar{\eta}_i$ -s of each experiments, are given in the first two columns of Tables 2 and 3. The presented numbers are the average of 40 tests, which are followed ± the standard deviation. We may observe that the highest standard deviation belongs to configuration a, where the unevenness of the surface affects the impact.

During the impacts it was observed that small slips (and a minor twisting) occurred, which means that part of the loss in energy is due to the slips and not due to the impact. In two cases, identified in Table 3 by an asterisk, the slip was significant.

By comparing the experiments to each other a few important observations can be made.

- (1) $\bar{\eta}_a < \eta_{\text{HousC}}$, as it was expected the energy loss in the experiment is much smaller than in Housner’s model (13.4 < 28.4; 12.4 < 17.7; Table 2).
- (2) $\bar{\eta}_a < \bar{\eta}_c$, i.e. when impacts are enforced to occur at the edge, the energy loss is higher than on the rocking block (12.4 < 19.5; Tables 2, 3). Note that significant slips occurred with configuration c for the lower aspect ratio during the motion, which explains the very high energy loss.
- (3) $\bar{\eta}_b < \bar{\eta}_c$, the energy loss is smaller if two impacts occurs instead of one (11.2 < 57.9; 6.9 < 19.5; Table 3).
- (4) $\bar{\eta}_c \simeq \eta_{\text{HousC}}$, if it is made sure that impact really occurs at the edges the difference between the experiments and Housner’s model is small at the slender block (19.5 > 17.2; Tables 2, 3).
- (5) $\bar{\eta}_a > \bar{\eta}_b$, an enforced impact at the middle decreases the loss in energy, note, however, that the difference is much smaller than in item 1 (11.2 < 13.4 < 28.4; 6.9 < 12.4 < 17.7; Tables 2, 3).

5 Model and verification

We extended Housner's rocking model with the following modifications:

- Impact may occur at an arbitrary position, not only at the corners. The equations corresponding to this modification are given in the “Appendix”.
- Several impacts may arise consecutively (see the “Appendix” for two consecutive impacts).

To follow the entire motion of the blocks, a simple computer code was developed to calculate the position, velocity and acceleration of the block at each step, while rocking was modeled with one or more consecutive impacts. The slips were not modeled.

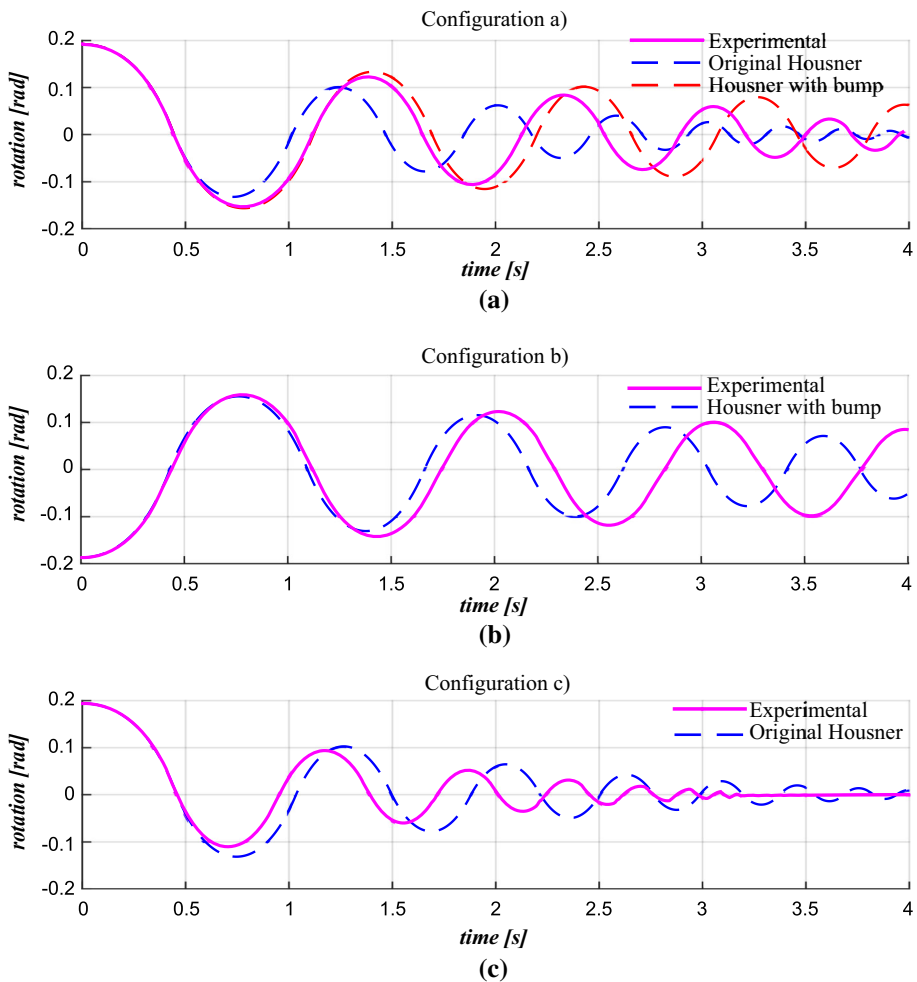


Fig. 11 Examples of the experimental results for configuration a, b and c, investigating the block with slenderness 3.7

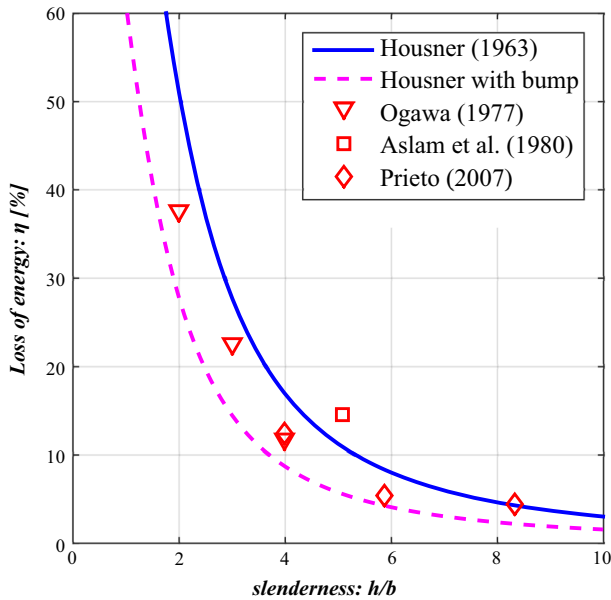


Fig. 12 Experimental results compared with the classical Housner's model and with the refined model including a bump in the middle

With these modifications the motion of the blocks with configurations b , c and d were also calculated. A typical example was shown in Fig. 10. The relative loss in energy is given in the last two columns of Table 3.

In every case the experimental values are 1–3% off the calculated value. That difference is much smaller than between the “classical” experiments (configuration a) and Housner's model (5–15%, see Table 2).

It is also an important observation that $\bar{\eta}_a > \bar{\eta}_b$, however, the difference is smaller than the difference between $\bar{\eta}_a$ and the classical Housner's model. It seems a reasonable approximation for the modeling of a rocking block that a bump is assumed at the middle of the block. According to our calculations and experiments this is a conservative approximation since this model underpredicts the loss of energy (while the classical Housner's model overpredicts it).

We tested this hypothesis with the experiments published by Ogawa (1977), Aslam et al. (1980), Prieto-Castrillo (2007), Elgawady et al. (2011). See Fig. 12, where the dashed line represents Housner's model with an extra bump in the middle.

Three further comparisons for configurations a , b and c are given in Fig. 11. For configurations b and c the change in the amplitudes in the experiments and the calculations are close to each other, while for configuration a the original Housner's model overpredicts the change in amplitude, and the modified underpredicts it.

6 Conclusion

In this paper we investigated the reasons of the well-known fact (see Figs. 3, 4) that experiments show lower energy loss during impact than it is predicted by Housner's model. It was found that the main reason for the difference is that in the original model the best

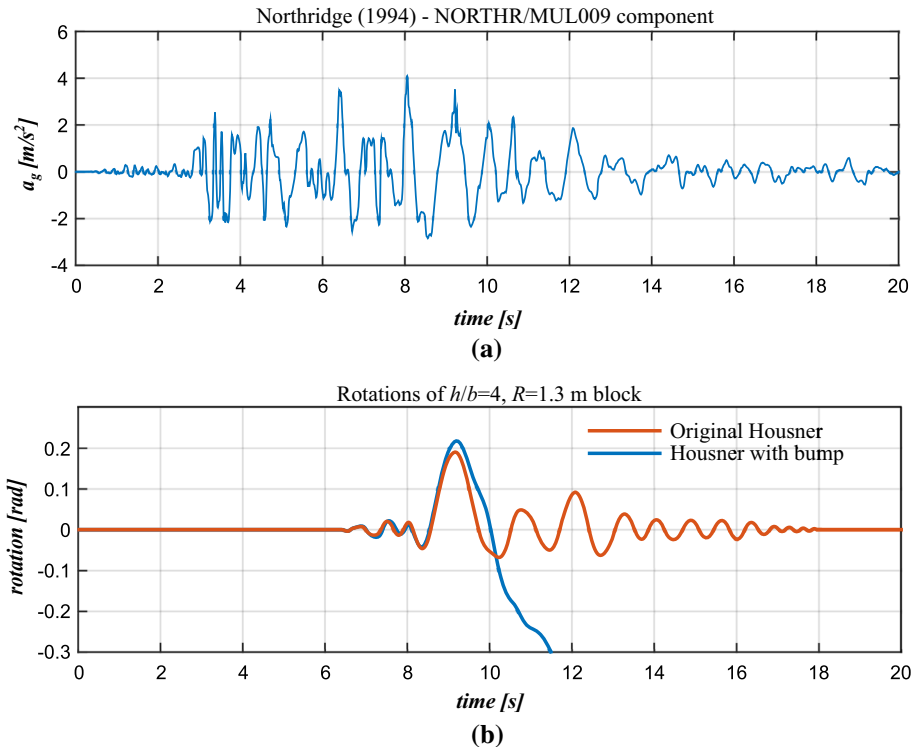


Fig. 13 The rocking motion of a block considering the original Housner's model and the proposed improvement

case scenario was assumed: that impact occurs at the edges (Fig. 7b), which results in the maximum energy loss. In reality, due to the unevenness of the surfaces, or due to the presence of aggregates between the interfaces, rocking may occur with consecutive impacts, which reduce the energy loss.

A simple possible phenomenological improvement of Housner's model is that one additional bump (and consequently an additional impact) is assumed in the middle of the section (Fig. 7c). This modified model is proposed to be taken into account, when masonry and stone columns and arches (Fig. 2) are analyzed.

To demonstrate the importance of the improvement of Housner's model a block was considered, which is subjected to a base excitation recorded at the Northridge earthquake shown in Fig. 13a (1994, NORTHTR/MUL009 component). The aspect ratio of the element is 4, while its diagonal is 2.6 m, hence its sizes are $b = 0.315$ m and $h = 1.261$ m. When Housner's classical model is applied (Fig. 13b) the block does not overturn, its maximum inclination is about 80% of the neutral position (at about 9 s). When the above improved model is applied (with one additional bump), which agrees better with the experiments, it can be observed that the inclination of the block becomes bigger and bigger during the excitation, resulting in overturning at about 11 s.

Acknowledgements This work is being supported by the Hungarian Scientific Research Fund (OTKA, No. 115673).

Appendix: Housner’s model when the two axes of rotation are at arbitrary locations

Here, we give the simple extension of Housner’s model, when the location of the axis of rotation before impact (P_1) and after the impact (P_2) are not at the edges of the block but at arbitrary positions (Fig. 14). Immediately before impact (rotation around axis P_1) the angular momentum about axis P_2 is

$$L_b = m\omega_b \left(\frac{(2b)^2}{12} + \frac{(2h)^2}{12} + h^2 + x_1x_2 \right), \tag{3}$$

while after impact (rotation around axis P_2) the moment of momentum about axis P_2 is:

$$L_a = m\omega_a \left(\frac{(2b)^2}{12} + \frac{(2h)^2}{12} + h^2 + x_2^2 \right), \tag{4}$$

where m is the mass of the block, and x_1 and x_2 are the locations of the axes measured from the middle of the edge. From the condition that $L_a = L_b$, we obtain the following expression for the angular velocity:

$$\omega_a = \mu\omega_b, \quad \mu = \frac{2h^2 + 0.5b^2 + 1.5x_1x_2}{2h^2 + 0.5b^2 + 1.5x_2^2}. \tag{5}$$

For $x_1 = -b$ and $x_2 = b$ Eqs. (1) and (5) are identical.

If the corners are cut (Fig. 14), and we set $x_1 = -b_2$ and $x_2 = b_2$, Eq. (5) results in

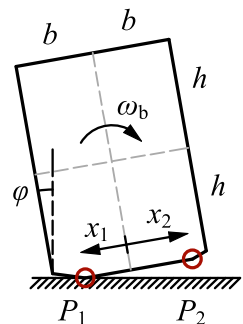
$$\omega_a = \mu_{\text{HousC}}\omega_b, \quad \mu_{\text{HousC}} = \frac{2h^2 + 0.5b^2 - 1.5b_2^2}{2h^2 + 0.5b^2 + 1.5b_2^2}. \tag{6}$$

Now we apply Eq. (5) in two steps. First, $x_1 = -b_2$ and $x_2 = 0$, i.e. the block rotates at the left corner and then impact occurs at the middle. Equation (5) gives:

$$\omega_{a1} = \omega_{b1}; \tag{7}$$

and second: $x_1 = 0$ and $x_2 = b_2$, i.e. the block rotates at the middle and then impact occurs at the right corner:

Fig. 14 Housner’s model for a rocking block if rotation occurs around two axes of arbitrary position



$$\omega_{a2} = \omega_{b2} \frac{2h^2 + 0.5b^2}{2h^2 + 0.5b^2 + 1.5b_2^2}. \quad (8)$$

By setting $\omega_a = \omega_{a2}$, $\omega_b = \omega_{b1}$, $\omega_{a1} = \omega_{b2}$, from Eqs. (7) and (8) we obtain an expression for the change in the angular velocity, if rocking occurs in two steps, according to the geometry shown in Fig. 7b:

$$\omega_a = \mu_{\text{HousC}}^{2\text{imp}} \omega_b, \quad \mu_{\text{HousC}}^{2\text{imp}} = \frac{2h^2 + 0.5b^2}{2h^2 + 0.5b^2 + 1.5b_2^2}. \quad (9)$$

If the width of the block is identical to the width of the base ($b = b_2$) Eq. (9) simplifies to

$$\omega_a = \mu_{\text{HousC}}^{2\text{imp}} \omega_b, \quad \mu_{\text{HousC}}^{2\text{imp}} = \frac{2h^2 + 0.5b^2}{2h^2 + 2b^2}. \quad (10)$$

Since the kinetic energy is proportional to the square of the angular velocity, the relative loss in kinetic energy during rocking can be calculated as:

$$\eta = \frac{\omega_b^2 - \omega_a^2}{\omega_b^2} = 1 - \mu^2, \quad (11)$$

where ω_b and ω_a are the angular velocities before and after rocking, and μ is the angular velocity ratio defined by Eqs. (1), (6), (9) and (10).

References

- Anooshehpour A, Brune JN (2002) Verification of precarious rock methodology using shake table tests of rock models. *Soil Dyn Earthq Eng* 22:917–922. doi:[10.1016/S0267-7261\(02\)00115-X](https://doi.org/10.1016/S0267-7261(02)00115-X)
- Aslam M, Godden WG, Scalise DT (1980) Earthquake rocking response of rigid bodies. *J Struct Div* 106:377–392
- Augusti G, Sinopoli A (1992) Modelling the dynamics of large block structures. *Meccanica* 27:195–211. doi:[10.1007/BF00430045](https://doi.org/10.1007/BF00430045)
- De Lorenzis L (2007) Failure of masonry arches under impulse base motion. *Earthq Eng Struct Dyn* 36:2119–2136. doi:[10.1002/eqe](https://doi.org/10.1002/eqe)
- Di Egidio A, Contento A (2009) Base isolation of slide-rocking non-symmetric rigid blocks under impulsive and seismic excitations. *Eng Struct* 31:2723–2734. doi:[10.1016/j.engstruct.2009.06.021](https://doi.org/10.1016/j.engstruct.2009.06.021)
- Elgawady M, Ma QTM, Butterworth JW, Ingham J (2011) Effects of interface material on the performance of free rocking blocks. *Earthq Eng Struct Dyn* 40:375–392. doi:[10.1002/eqe.1025](https://doi.org/10.1002/eqe.1025)
- Hogan SJ (1989) On the dynamics of rigid-block motion under harmonic forcing. *Proc R Soc A Math Phys Eng Sci* 425:441–476. doi:[10.1098/rspa.1989.0114](https://doi.org/10.1098/rspa.1989.0114)
- Housner G (1963) The behavior of inverted pendulum structures during earthquakes. *Bull Seismol Soc Am* 53:403–417
- Kounadis AN (2015) On the rocking–sliding instability of rigid blocks under ground excitation: some new findings. *Soil Dyn Earthq Eng* 75:246–258. doi:[10.1016/j.soildyn.2015.03.026](https://doi.org/10.1016/j.soildyn.2015.03.026)
- Lagomarsino S (2015) Seismic assessment of rocking masonry structures. *Bull Earthq Eng* 13:97–128. doi:[10.1007/s10518-014-9609-x](https://doi.org/10.1007/s10518-014-9609-x)
- Lipscombe PR, Pellegrino S (1993) Free rocking of prismatic blocks. *J Eng Mech* 119:1387–1410. doi:[10.1061/\(ASCE\)0733-9399\(1993\)119:7\(1387\)](https://doi.org/10.1061/(ASCE)0733-9399(1993)119:7(1387))
- Ma QTM (2010) The mechanics of rocking structures subjected to ground motion. The University of Auckland, Auckland
- Makris N, Konstantinidis D (2003) The rocking spectrum and the limitations of practical design methodologies. *Earthq Eng Struct Dyn* 32:265–289. doi:[10.1002/eqe.223](https://doi.org/10.1002/eqe.223)

- Makris N, Vassiliou MF (2012) Sizing the slenderness of free-standing rocking columns to withstand earthquake shaking. *Arch Appl Mech* 82:1497–1511. doi:[10.1007/s00419-012-0681-x](https://doi.org/10.1007/s00419-012-0681-x)
- Ogawa N (1977) A study on rocking and overturning of rectangular column. In: Report of the National Research Center for disaster prevention (18) 14
- Oppenheim I (1992) The masonry arch as a four-link mechanism under base motion. *Earthq Eng Struct Dyn* 21:1005–1017
- Priestley MJN, Evison RJ, Carr AJ (1978) Seismic response of structures free to rock on their foundations. *Bull N Z Soc Earthq Eng* 11:141–150
- Prieto F (2007) On the dynamics of rigid-block structures applications to SDOF masonry collapse mechanisms. GUIMARÃES. University of Minho, Braga
- Prieto F, Lourenço PB, Oliveira CS (2004) Impulsive Dirac-delta forces in the rocking motion. *Earthq Eng Struct Dyn* 33:839–857. doi:[10.1002/eqe.381](https://doi.org/10.1002/eqe.381)
- Psycharis IN (1990) Dynamic behaviour of rocking two-block assemblies. *Earthq Eng Struct Dyn* 19:555–575. doi:[10.1002/eqe.4290190407](https://doi.org/10.1002/eqe.4290190407)
- Psycharis IN, Papastamatiou DY, Alexandris AP (2000) Parametric investigation of the stability of classical columns under harmonic and earthquake excitations. *Earthq Eng Struct Dyn* 29:1093–1109. doi:[10.1002/1096-9845\(200008\)29:8<1093:AID-EQE953>3.0.CO;2-S](https://doi.org/10.1002/1096-9845(200008)29:8<1093:AID-EQE953>3.0.CO;2-S)
- Shi B, Anooshehpour A (1996) Rocking and overturning of precariously balanced rocks by earthquakes. *Bull Seismol Soc Am* 86:1364–1371
- Spanos PD, Roussis PC, Politis NPA (2001) Dynamic analysis of stacked rigid blocks. *Soil Dyn Earthq Eng* 21:559–578. doi:[10.1016/S0267-7261\(01\)00038-0](https://doi.org/10.1016/S0267-7261(01)00038-0)
- Ther T, Kollár LP (2014) Response of masonry columns and arches subjected to base excitation. In: Ansal A (ed) Second European conference on earthquake engineering and seismology. Istanbul
- Voyagaki E, Psycharis IN, Mylonakis G (2013) Rocking response and overturning criteria for free standing rigid blocks to single-lobe pulses. *Soil Dyn Earthq Eng* 46:85–95. doi:[10.1016/j.soildyn.2012.11.010](https://doi.org/10.1016/j.soildyn.2012.11.010)
- Zulli D, Contento A, Di Egidio A (2012) 3D model of rigid block with a rectangular base subject to pulse-type excitation. *Int J Non Linear Mech* 47:679–687. doi:[10.1016/j.ijnonlinmec.2011.11.004](https://doi.org/10.1016/j.ijnonlinmec.2011.11.004)